The RXLR-EER Motif Determines an Unconventional Secretion Pathway Associated with Extracellular Vesicle Production

Wei Wang[1]*, Shumei Wang[1]*§, Lin Xu[1, 2], Lydia Welsh[3], Petra C Boevink[3], Steve C Whisson[3] & Paul RJ Birch[1,3]§.

[1] Division of Plant Sciences, School of Life Science, University of Dundee (at James Hutton Institute), Invergowrie, Dundee DD2 5DA, United Kingdom;

[2] Cell and Developmental Biology Department, John Innes Centre Norwich Research Park, Norwich, United Kingdom;

[3] Department of Cell and Molecular Sciences, James Hutton Institute, Invergowrie, Dundee DD2 5DA, United Kingdom;

* These authors contributed equally to this work

§ Authors for correspondence: P.Birch@dundee.ac.uk; swang002@dundee.ac.uk

Abstract

Phytophthora infestans, the cause of potato late blight disease, delivers a suite of RXLR effectors into host plant cells to subvert immunity, whereas apoplastic effectors act extracellularly. Although RXLR-EER motifs are critical for host translocation and are cleaved prior to secretion, the relevance of this processing is poorly understood. Prior evidence suggests RXLR effectors utilize a distinct, unconventional secretion pathway, raising the question of whether the RXLR-EER motifs influence selection of the secretion route. Here, we combined genetic, molecular and cell biology approaches to investigate the secretion pathways of RXLR effectors. Confocal microscopy revealed that RXLR and apoplastic effectors localize to distinct vesicular compartments in cultured hyphae. Moreover, fusing the ER retention signal KDEL to RXLR effectors did not impair their secretion, in contrast to apoplastic effectors, which were retained in the endomembrane system, indicating that RXLR effectors bypass the canonical ER-to-Golgi pathway. Importantly, RXLR effectors associate with extracellular vesicles, whereas RXLR-EER motif mutants show reduced association and are rerouted through the ER-to-Golgi secretion pathway. These findings demonstrate that the RXLR-EER motif governs effector sorting into an unconventional, EV-linked secretion route. This study sheds light on the molecular basis of effector trafficking in *P. infestans* and underscores the potential role of EVs in delivering virulence factors during host colonization.

Introduction

The oomycete *Phytophthora infestans* is the causative agent of potato late blight, a devastating disease that triggered the Irish potato famine in the 19th century and continues to pose a major threat to global food security [1, 2]. As a highly adapted hemi-biotrophic pathogen, *P. infestans* relies on a large and complex suite of effector proteins to manipulate host cell physiology and suppress immune responses, enabling successful colonization and disease progression.

The effectors can be broadly divided into two classes based on their site of action: apoplastic effectors, which are secreted into the extracellular space (apoplast) [3], and cytoplasmic effectors with an Arg-any amino acid-Arg-Leu (RXLR) motif, many of which have followed closely by

EER (Glu-Glu-Arg) motif, downstream of a secretion signal peptide are encoded by hundreds of genes within the genomes of *Phytophthora* spp. and downy mildew pathogens [4, 5, 6]. RXLR effectors are delivered into the host cell cytosol and target multiple proteins and processes at diverse locations inside host cells to suppress immunity [7, 8, 9, 10]. Whereas apoplastic effectors may be perceived by host pattern recognition receptors (PRRs) at the cell surface, RXLR effectors interfere with intracellular immunity by targeting various host processes within plant cells and can, in turn, be perceived by nucleotide-binding leucine-rich repeat receptors [11]. The RXLR-EER motif is crucial for host cell translocation and is proteolytically cleaved prior to secretion, although the functional consequences of this processing are poorly understood [12, 13, 14].

Previous studies show that apoplastic effectors in *P. infestans* are secreted via the conventional ER-to-Golgi pathway, as indicated by their sensitivity to the inhibitor brefeldin A (BFA). In contrast, RXLR effectors are largely BFA-insensitive, suggesting they follow an unconventional secretion route[15, 16]. A similar dichotomy in effector secretion has been observed in the fungal pathogen *Magnaporthe oryzae*, where cytoplasmic effectors are delivered via a BFA-insensitive, non-classical pathway, while apoplastic effectors rely on BFA-sensitive ER-to-Golgi trafficking [17]. However, it is important to recognise that BFA treatment can have off-target or pleiotropic effects, including disruption of endosomal trafficking, vesicle recycling, and broader alterations in membrane dynamics [18]. These side-effects may complicate interpretation of BFA sensitivity assays, particularly in complex filamentous pathogens such as *P. infestans*, where multiple secretory routes may coexist. Therefore, while BFA sensitivity provides a useful initial indication of secretory pathway involvement, additional genetic and imaging-based approaches are essential to unambiguously distinguish between conventional and unconventional secretion routes.

Recently, emerging evidence suggests that RXLR effectors are secreted via an unconventional pathway potentially associated with production of extracellular vesicles (EVs)[19]. EVs are membrane-bound nanoparticles released by cells into the extracellular milieu and have been increasingly recognized as vehicles for intercellular communication and molecular cargo delivery between organisms from different kingdoms[20]. Recently, EVs have been shown to play a pivotal bidirectional transport role in plant–pathogen interactions [21, 22, 23, 24, 25]. In addition to the intriguing link between EVs and effector trafficking, the mechanisms by which RXLR effectors are sorted to EVs, and the signals that determine their route of secretion, are largely unknown. In particular, whether the RXLR-EER motif influences intracellular sorting within the pathogen secretory systems has yet to be resolved.

In this study, we combined molecular, genetic and live-cell imaging approaches to investigate the secretion pathway of RXLR effectors in *P. infestans*. To determine whether these effectors utilize the classical ER–to-Golgi secretion route, we fused a canonical ER retention signal, KDEL (Lys-Asp-Glu-Leu), to RXLR effectors. The KDEL motif, typically found at the C-terminus of ER-resident proteins, is recognized by KDEL receptors in the cis-Golgi, which mediate the retrograde transport of these proteins back to the ER. While apoplastic effectors were largely retained in the ER after the addition of KDEL, RXLR effectors remained efficiently secreted, suggesting that they bypass the conventional ER–Golgi pathway. Furthermore, site-directed mutagenesis of the RXLR-EER motifs redirected these effectors to the classical ER-to-Golgi secretion route and disrupted their association with EVs, indicating that the RXLR-EER motif plays a role in effector trafficking within the pathogen.

Our findings provide compelling evidence that the RXLR-EER motif governs effector trafficking within *P. infestans*, channelling them into an unconventional secretory route linked to EV production. This study deepens our understanding of effector biogenesis and secretion

and highlights EVs as potential mediators of virulence protein delivery in plant-pathogen interactions.

Results

RXLR effectors and apoplastic effectors are associated with different types of trafficking vesicles

Previous studies have shown that the secretion of RXLR effectors in *P. infestans* is largely insensitive to BFA, whereas the secretion of apoplastic effectors is BFA-sensitive. This differential response suggests that RXLR and apoplastic effectors utilize distinct secretion pathways [15, 16]. To further explore this hypothesis, we co-expressed two apoplastic effectors, PiSCR74 and PiEPIC1, each C-terminally tagged with fluorescent proteins (mCitrine or mCherry respectively), in *P. infestans* and analyzed their localization using confocal microscopy. The two proteins exhibited substantial co-localization in puncta in cultured hyphae, consistent with the previous observations[15, 16] that they are both trafficked through the conventional secretory pathway (Fig. 1a). We have shown that RXLR effectors Pi04314 and Pi09216 strongly co-localized in cultured hyphae[19]. Consistent with these findings, co-expression of Pi04314 and PiAVRblb1 also revealed robust co-localization, reinforcing the concept that RXLR effectors follow a common intracellular trafficking route (Extended Data Fig. 1a). In contrast, when apoplastic effector PiSCR74 was co-expressed with RXLR effector Pi04314, the two proteins localized to distinct subcellular compartments, providing supporting evidence that RXLR and apoplastic effectors are sorted through different secretory routes (Fig. 1b).

To investigate whether these effectors are associated with distinct populations of endosomal vesicles, we isolated endo-vesicles from cultured mycelia using a sucrose gradient that was bottom-loaded to allow vesicles to rise to their buoyant density and thus exclude protein aggregates (Extended Data Fig. 1b). Transmission electron microscopy of the vesicle fractions (VFs) confirmed the presence of typical membrane-bound vesicles (Extended Data Fig. 1c). Confocal imaging of the VFs revealed that fluorescent protein tagged PiSCR74 and PiEPIC1 largely co-localized within the same vesicle population. Furthermore, fluorescence signals from both effector fusions were abolished by pre-treatment with 1% TritonX-100 detergent, which disrupts lipid membranes but not protein aggregates[26, 27] (Fig. 1c). Similarly, two fluorescently tagged RXLR effectors Pi04314 and PiAVRblb1 largely co-localized within the same vesicle population (Extended Data Fig. 1d). In contrast, Pi04314 and PiSCR74 fusions localized to separate vesicle populations. Similarly, their respective fluorescence signals were also detergent-sensitive, indicating membrane association (Fig. 1d). Immunoblot analysis confirmed that apoplastic and RXLR effectors were all present in the vesicle fractions, and that detergent treatment abolished their presence in VFs (Extended Data Fig. 1e). These results indicate their association with membrane-bound vesicular structures, supporting the conclusion that RXLR and apoplastic effectors are sorted into distinct vesicle types and follow different secretion pathways in *P. infestans*.

RXLR effectors follow a Golgi-independent route after cleavage

Given that apoplastic effectors are secreted via the conventional ER-to-Golgi pathway and that RXLR effectors are insensitive to BFA treatment, we hypothesized that RXLR effectors utilize a Golgi-bypass secretion mechanism. To test this hypothesis, we employed a molecular strategy involving the addition of an ER retention signal—KDEL (Lys-Asp-Glu-Leu)—to the C-terminus of effector-fluorescent protein fusions. The KDEL motif is recognized by KDEL receptors (KDELRs) located in the cis-Golgi, which mediate retrograde transport of KDEL-

138 tagged proteins back to the ER [28]. Proteins secreted via a Golgi-independent route are expected
139 to escape this retention mechanism. To evaluate this, apoplastic (PiSCR74 and PiEPIC1) or
140 RXLR (Pi04314 and PiAVRblb1) effector fluorescence protein fusions either with or without
141 the KDEL motif, were expressed in *P. infestans* strains cultured in liquid medium.
142 Immunoblotting revealed that apoplastic effectors were efficiently secreted under normal
143 conditions, but their secretion was markedly reduced upon addition of KDEL, whereas the
144 secretion of RXLR effectors was largely unaffected, indicating that their export does not
145 primarily depend on Golgi-mediated trafficking (Fig. 2a).

146 We validated these findings *in planta* using confocal microscopy. All effectors accumulated at
147 the haustorial interface under normal conditions. However, upon KDEL addition, apoplastic
148 effectors accumulated in ER-like endomembrane compartments, consistent with receptor-
149 mediated retention. In contrast, RXLR effectors accumulated at the haustorial interface even
150 when fused to KDEL (Fig. 2b). These results strongly support the conclusion that apoplastic
151 effectors are secreted through a conventional ER-Golgi pathway, whereas RXLR effectors are
152 exported via a Golgi-bypass mechanism.

153 Our previous work showed that the RXLR-EER motif is not recognized or correctly cleaved in
154 plant cells[14]. To determine whether proteolytic processing of this motif influences the pathway
155 of secretion, the RXLR effector Pi04314 — with or without its native signal peptide (SP) —
156 was transiently expressed in *Nicotiana benthamiana*. Confocal microscopy revealed that the
157 SP-containing version was secreted into the apoplast, whereas the version lacking the SP
158 localized to the nucleus or nucleolus, the expected site of the effector activity *in planta* [29, 30].
159 While BFA treatment disrupted secretion of SP-tagged Pi04314, causing it to accumulation in
160 BFA bodies[31], it did not alter the subcellular localization of NSP-Pi04314 (Extended Data Fig.
161 2a). Addition of a C-terminal KDEL motif caused SP-04314-RFP to be retained in the ER
162 (Extended Data Fig. 2b), confirming that uncleaved RXLR effectors follow the conventional
163 ER-Golgi pathway in plant cells. These results highlight the importance of appropriate
164 recognition and cleavage of the RXLR-EER motif in directing these effectors toward an
165 alternative, Golgi-bypass secretion route.

166 **The RXLR-EER motif determines the secretion pathway.**

167 Given that the RXLR-EER motif functions as a protease processing site prior to secretion [13, 14],
168 we sought to investigate whether this motif also determines the secretion route of RXLR
169 effectors. In previous work, we showed that RXLR-EER motif mutants could still be secreted
170 at haustoria[14], but it is unclear if the secretion pathway was altered. To test this, we generated
171 a mutant version of the RXLR effector Pi04314 in which the RXLR-EER motif was substituted
172 with alanines (Pi04314-7A). Both wild-type (WT) and mutant versions were fused with
173 different fluorescent proteins (mCherry or mCitrine) and co-expressed in *P. infestans*. Confocal
174 microscopy of cultured hyphae revealed that the WT and mutant effectors localized to distinct
175 vesicular compartments (Fig. 3a). Notably, the Pi04314-7A mutant co-localized significantly
176 with apoplastic effector PiSCR74 (Fig. 3b), suggesting a shift in its trafficking route. Endo-
177 vesicle isolation from the same transformants confirmed that the RXLR-EER mutant was
178 sorted into vesicles distinct from those carrying the wild-type RXLR effectors (Fig. 3c), but
179 largely co-localized with vesicles associated with apoplastic effector PiSCR74 (Fig. 3d).
180 Importantly, addition of a KDEL motif to the RXLR-EER 7A mutants, for both Pi04314 and
181 PiAVRblb1, significantly impaired their secretion into the culture medium (culture filtrate, CF)
182 (Fig. 3e, Extended Data Fig. 3a). *In planta*, these KDEL-tagged mutants displayed ER retention
183 patterns similar to those observed for KDEL-tagged apoplastic effectors (Fig. 3f, Extended
184 Data Fig. 3b). These findings indicate that the RXLR-EER motif plays a key role in directing

185 RXLR effectors into an unconventional, Golgi-independent secretion pathway, and its mutation
186 leads to conventional ER-to-Golgi secretion.

187 **The RXLR-EER motif govern the association of RXLR effectors with EVs**

188 Our recent work suggested that RXLR effectors such as Pi04314 and PiAVRblb1 are associated
189 with pellets containing EVs[19]. Pi04314 was also shown to co-localize, prior to secretion, with
190 two candidate EV markers, PiMDP1 and PiMDP2 in hyphal endo-vesicles[19]. To investigate
191 whether the RXLR-EER motif governs this co-association, we examined WT and RXLR-EER
192 mutant versions of the effectors (Pi04314-7A and PiAVRblb1-7A) using EVs isolated from
193 cultured mycelia and western blotting. Although the mutants were still detected in pellets
194 containing EVs, their abundance that relative to total secretion (CF) was significantly reduced
195 compared to the WT proteins, indicating diminished association with EVs (Fig. 4a). In contrast,
196 the addition of a C-terminal KDEL motif to the WT Pi04314 or PiAVRblb1did not affect EV
197 association (Fig. 4a), consistent with our findings that KDEL does not alter the secretion route
198 of RXLR effectors (Fig. 2a, b).

199 To further assess the role of the RXLR-EER motif in EV targeting, Pi04314-7A was co-
200 expressed with the EV marker PiMDP1 in *P. infestans*. Confocal microscopy showed no co-
201 localization between the mutant and PiMDP1 in cultured hyphae, and they were found in
202 distinct endo-vesicle populations (Fig. 4b, c; Extended Data Fig. 4a). In contrast, WT Pi04314
203 strongly co-localized with PiMDP1 in the same endo-vesicle types (Extended Data Fig. 4b, c).
204 Together, these findings demonstrate that the RXLR-EER motif and its processing are key
205 determinantS of RXLR effector sorting into an unconventional secretion pathway associated
206 with EV production.

207

208 **Discussion**

209 Our study provides compelling cell biological and genetic evidence that *P. infestans* deploys
210 distinct secretion pathways for two major classes of effector proteins—apoplastic and RXLR-
211 type cytoplasmic effectors. Whereas apoplastic effectors are secreted via the conventional ER-
212 to-Golgi pathway, RXLR effectors utilize an unconventional secretion route that bypasses the
213 Golgi. Critically, we demonstrate that the RXLR-EER motif is essential for determining the
214 unconventional secretion of these cytoplasmic effectors and their association with extracellular
215 vesicles (EVs).

216 Previously, sensitivity to the inhibitor BFA was used to distinguish between *P. infestans*
217 apoplastic and cytoplasmic (RXLR) effector secretion pathways [15, 16]. This approach was used
218 also to demonstrate that apoplastic and cytoplasmic effectors from the fungal pathogen of rice
219 and wheat, *Magnaporthe oryzae*, were also secreted by conventional and unconventional
220 pathways, respectively [17]. However, BFA treatment can have off-target effects [18]. As such, non-
221 disruptive cell biological and genetic approaches are required to confirm inhibitor-based
222 studies. We found that apoplastic effectors and RXLR effectors did not co-localise at mobile
223 endo-vesicles in *P. infestans* hyphae (Fig 1), consistent with their secretion via different
224 pathways. Critically, whereas addition of a KDEL motif to the C-terminus of apoplastic
225 effectors resulted in their retention in hyphae, consistent with retrograde trafficking of them
226 from the Golgi to the ER, addition of a KDEL motif to RXLR effectors did not prevent their
227 secretion (Fig 2). These cell biological and genetic approaches, which agree with previously
228 published BFA results [15,16], offer a non-disruptive means to distinguish between conventional
229 and unconventional secretion pathways that could be adopted to verify previous findings in
230 other fungi such as *M. oryzae* [17] and investigate effector secretion in other pests and pathogens
231 of plants or animals.

232 Importantly, we identified the RXLR-EER motif as a key determinant of unconventional
233 secretion of these effectors. Mutating the RXLR-EER motif not only altered the intracellular
234 localization of RXLR effectors—leading them to co-localize in endo-vesicles with apoplastic
235 effectors—but also shifted their secretion to a Golgi-dependent route (Fig. 3). When the RXLR-
236 EER motif was mutated, effectors were retained in the ER upon addition of a KDEL tag,
237 confirming they were secreted conventionally via the Golgi (Extended Data Fig. 2). We thus
238 argue that the RXLR-EER motif acts as an ER sorting signal to an unconventional, Golgi-
239 bypass secretion path. Importantly, secretion of the WT RXLR effector Pi04314-mRFP by the
240 plant *N. benthamiana* followed a conventional ER-to-Golgi pathway that was BFA-sensitive
241 and prevented by addition of a KDEL motif (Extended Data Fig. 2). As we showed previously
242 that there is no efficient proteolytic cleavage of Pi04314 during secretion by *N. benthamiana*[14]
243 this strongly implicates such processing of the RXLR-EER motif as a requirement for sorting
244 into an unconventional secretion pathway. Interestingly, our recent observation that RXLR
245 effectors are often associated with extracellular vesicles (EVs), whereas apoplastic effectors
246 are not[19], provides further evidence that these effector classes follow distinct secretion
247 pathways. Our data here demonstrate that the RXLR-EER motif also governs the association
248 of RXLR effectors with EVs. Whereas WT RXLR effectors co-localized with EV markers and
249 were enriched in EV pellets, their RXLR-EER mutants showed diminished EV-association and
250 failed to co-localize with EV markers (Fig. 4, Extended Data Fig. 4). This suggests that the
251 RXLR-EER motif has a critical role in the intracellular sorting of RXLR effectors toward an
252 unconventional pathway associated with EV production.

253 The *Phytophthora* RXLR effectors have been described as analogous to PEXEL effectors
254 delivered into human cells by the distantly-related apicomplexan malaria pathogen
255 *Plasmodium falciparum* [32]. PEXEL effectors contain a related motif, RxLxE/D/Q, which is also
256 proteolytically processed during secretion [33]. The precise role of this motif remains unclear.
257 Our findings reveal a role for the RXLR-EER motif in directing RXLR effectors to an
258 unconventional secretion pathway that bypasses the Golgi following proteolytic cleavage. This
259 is different to PEXEL effectors from *Plasmodium* which, following proteolytic cleavage in the
260 ER, are secreted through the ER-to-Golgi pathway [34]. Future studies should focus on
261 identifying the molecular machinery that processes RXLR-EER motifs within *Phytophthora*
262 and mediates their sorting into an unconventional secretion pathway associated with EV
263 production. This machinery could represent a novel target for disease control.

264

265 **Methods**

266 ***Phytophthora infestans* growth and plant growth**

267 *Phytophthora infestans* (*P. infestans*) strain 3928A, along with its derived transgenic lines, was
268 cultured on Rye Agar medium supplemented with Ampicillin (100 µg/ml) and Pimaricin
269 (0.02%). Geneticin (10 µg/ml) was included to ensure the selection and maintenance of
270 transgenic lines. *Nicotiana benthamiana* and the susceptible potato cultivar Solanum
271 tuberosum 'Maris Piper' were grown in controlled glasshouse conditions under a 16-hour
272 light/8-hour dark cycle.

273 To assess the secretion efficiency of *P. infestans*. A 14-day old plate was flooded with 3ml
274 amended lima bean (ALB) liquid media supplemented with the appropriate antibiotics scraped
275 with a sterile spreader and grown for 1 days in the dark without shaking. Mycelia were
276 transferred into fresh culture tubes containing 1.5 ml ALB (with appropriate antibiotics) which
277 had been pre-cleared by ultracentrifugation at 120 000 × g for 2 hours. Cultures were grown
278 for a further day.

For EV/Endo-vesicle isolation. At least two 14-day old plates were flooded with 15ml amended lima bean (ALB) liquid media supplemented with the appropriate antibiotics. Sporangia were collected by pouring the suspension into a sterile culture bottle through a 70 µm cell strainer. Sporangia were allowed to grow for 2 days (or 4 days for endo-vesicle isolation) in the dark without shaking. To isolate EVs, mycelia were transferred into fresh culture bottles containing 15 ml minimal media and 15 ml ALB which had been pre-cleared by ultracentrifugation at 120, 000*g* for 2 h. Cultures were grown for a further 2 days.

Construction of *P. infestans* transgenic lines

The vector pmCitrine:mCherry, designed for co-expression of proteins tagged with mCitrine and mCherry, was constructed by Breen et al., (2025)[19]. The coding sequence for PiSCR74 was amplified from a published vector[35]. Coding sequences for PiEPIC1 (PITG_09169) and Pi04314 (PITG_04314) were amplified from published vectors constructed by Wang et al., (2017, 2018)[15, 16], and PiAVRblb1 (PITG_21388) and all RXLR-EER mutated versions were amplified from published vector generated by Xu et al., (2025)[14], using primers listed in Extended Table 1. KDEL motif was synthesised with restriction enzyme sites (Extended data table 1). These coding sequences were cloned as C-terminal fusions to the fluorescent proteins, driven by the oomycete Ham34 promotor (Ham34P)[36], using restriction enzyme cloning and standard molecular biology techniques. Plasmids were sequenced to verify the correct insertion of target sequences and prepared for downstream applications using the Promega PureYield™ Plasmid Maxiprep System. Transformation of *P. infestans* isolate 3928A was conducted following the protocol described by Welsh et al. (2025)[37].

Construction of expression vectors and transient expression *in planta*

The *P. infestans* genes encoding Pi04314, PiSCR74, or PiAVRblb1, including their native predicted signal peptides and C-terminally fused mCherry, with or without a KDEL motif, were amplified from above constructed vectors used in *P. infestans* transformations. The vector lacking the signal peptide (NSP-Pi04314-mRFP) was generated by Wang et al. (2017)[15], while the NSP-PiAVRblb1-mRFP construct was produced by Xu et al. (2025)[14]. Gene-specific primers containing flanking Gateway recombination sites were used for PCR amplification (Extended data table 1). The purified PCR products were recombined into the entry vector pDONR201 (Invitrogen) to generate entry clones. These entry clones were subsequently recombined with the binary vector pK7WG2 and transformed into *Agrobacterium tumefaciens* strain GV3101 for transient expression in *Nicotiana benthamiana*[38]. *A. tumefaciens* cultures were infiltrated at an OD_{600} of 0.05. Brefeldin A (BFA) was applied at a final concentration of 20 µg/mL, 30–60 minutes prior to imaging, as previously described Wang et al., (2017)[15].

Immunoblotting and quantification

For protein extraction from *P. infestans* mycelia, approximately 0.01 g of fresh mycelium was collected in a 1.5 ml Eppendorf tube and mixed with 80 µl of 2× SDS buffer (to assess the overall secretion efficiency, all obtained mycelia were collected in a 1.5 ml Eppendorf tube and ground with a pestle in 150 µl of 2× SDS buffer.). The sample was vortexed for 1 minute and subsequently boiled at 95°C for 10 minutes. For protein extraction from culture filtrate and supernatant, total proteins were isolated using the chloroform/methanol precipitation method[39]. Briefly, 4 ml of methanol, 1 ml of chloroform, and 4 ml of sterile water were added to 1 ml of liquid samples. To assess the overall secretion efficiency, all resulted culture filtrate (~1.5 ml) was used for precipitation. The mixture was thoroughly vortexed and centrifuged at 5000 × g for 20 minutes. The precipitated proteins were washed with 3 ml of absolute methanol, and the air-dried pellet was resuspended in 80 µl of 2× SDS loading buffer.

Samples were loaded onto 10% SDS-PAGE gels and transferred onto nitrocellulose membranes. Membranes were blocked for one hour at room temperature in 4% milk dissolved in 1× PBST (0.05% Tween 20). Primary antibodies targeting RFP/mCherry (Chromotek, 58F) and GFP/mCitrine (Roche, 11814460001) were diluted to 1:4000 and 1:2000, respectively, in blocking buffer and incubated with the membranes overnight at 4°C or room temperature for 2 hours. Following incubation, membranes were washed five times (10 minutes for each time) with 1× PBST. Secondary antibodies—IRDye® 680RD Goat anti-Rat IgG, IRDye® 800CW Goat anti-Mouse IgG (LI-COR Biosciences)—were added at a 1:5000 dilution in blocking buffer. Membranes were incubated with secondary antibodies for one hour at room temperature in the dark. Signal detection and quantification were performed using the LI-COR ODYSSEY® DLx imaging system and LICOR Image Studio™ software.

Endo-vesicles isolation from *P. infestans*

Endo-vesicles from *P. infestans* were isolated using 1–2 g of mycelia homogenized in an equal volume of isolation buffer (150 mM Na-HEPES, pH 7.5, 10 mM EDTA, 10 mM EGTA, 17.5% [w/w] sucrose, 7.5 mM KCl, 10 mM DTT, 1× PIC-W, 1× PIC-D, and 1× E-64) as described by Wang et al. (2023)[40]. For samples designated for Triton X-100 treatment, the supernatant was divided into two equal volumes. One portion was treated with Triton X-100 to a final concentration of 1%, while the other received an equivalent volume of sterile distilled water as a control. All samples were thoroughly mixed and incubated on ice for one hour. After incubation, the samples were adjusted to 40.6% (w/w) sucrose by mixing with 62% (w/w) sucrose solution. A 2.4 mL aliquot of this sucrose mixture was loaded at the bottom of a 13.2 mL ultracentrifuge tube and overlaid sequentially with 3 mL of 35% (w/w) sucrose, 3 mL of 25% (w/w) sucrose, and 3 mL of 8.5% (w/w) sucrose to form a gradient. The loaded gradient was centrifuged at 400,000*g* for 3 hours at 4 °C using a Beckman Coulter SW 41 Ti rotor. The two interfaces between the 8.5% and 25%, 25% and 35% sucrose layers was carefully collected and pelleted by ultracentrifugation at 100,000*g* for 1 hour at 4 °C. Pellets were prepared for microscopy analysis and immunoblotting. All sucrose solutions were prepared in 150 mM Na-HEPES buffer (pH 7.5) and included protease inhibitors (1× PIC-W, 1× PIC-D, and 1× E-64) to ensure vesicle integrity.

Transmission microscopy (TEM)

25 µl of endo-vesicle samples or buffer control was mixed with 25 µl of 4% paraformaldehyde (PFA) in 0.1 M sodium phosphate pH 7.4 to give a final concentration of 2% PFA. 30 µl aliquots were pipetted onto Parafilm with nickel grids (carbon-coated, formvar, 300 mesh) placed on top, and incubated at room temperature for 30 minutes. Grids were washed with 1x PBS twice and incubated for 10 minutes with 50µl 1% glutaraldehyde. Grids were then washed with 100 µl sterile water seven times and stained with 4% uranyl oxalate for 10 minutes at room temperature. Grids were transferred onto two 50 µl drops of uranyl acetate (0.15% methylcellulose and 0.4% uranyl acetate) sequentially and left on the second drop for 10 minutes on ice. Excess liquid was wicked off with filter paper and grids were inspected with a JEOL 1400 at 80 kV.

Confocal microscopy and data quantification

P. infestans hyphae grown in ultracentrifugation cleaned ALB medium on microscope slides were imaged at 1–2 days post-inoculation, while leaf infections on *Solanum tuberosum* were imaged at 2–3 days post-inoculation. *N. benthamiana* leaves were imaged at 2 days after *Agrobacterium* infiltration. Imaging was performed using a Nikon A1R confocal microscope.

For GFP fluorescence, the 488 nm line from an argon laser was used for excitation, and emissions were collected between 500–530 nm. For mCitrine fluorescence, the 514 nm line

from an argon laser was used for excitation, and emissions were collected between 520–550 nm. For mCherry fluorescence, a 561 nm laser was used for excitation, with emissions collected between 600–630 nm. The pinhole was set to 1.2 airy unit to optimize resolution. Images were processed using OMERO, or ImageJ software. To assess the effector secretion efficiency during infection, haustoria and adjacent area of invasive hyphae were chosen from single optical sections for measurement. The Fiji plugin DiAna was used for endo-vesicle co-localization analyses[41].

EV isolation from *P. infestans* culture

EVs were isolated from *P. infestans* culture as described before[19]. Approximately 30 ml culture was used for EV isolation. 1 ml of culture filtrate (CF) was collected after the removal of mycelia using a 70 µm cell strainer. The filtered CF was centrifuged for 10 minutes at 2000*g* and filtered through a 0.45 µm syringe filter, following a further spin at 10,000*g* for 30 minutes to remove all cellular debris and large vesicles. Supernatant from previous step was then ultracentrifuged at 100,000*g* for 1 hour at 4 °C (Beckman Coulter Type50.2 Ti rotor) to finally obtain the crude EV pellet (P) samples, pellet was dissolved in 80 µl SDS buffer for western blot.

Acknowledgements

We are grateful to colleagues Drs Hazel McLellan and Susan Breen for helpful discussions during the development of this research. We thank Dr Kasia Mackinnon for technical support. The research was supported by United Kingdom Research and Innovation Horizon Europe Guarantee Marie Skłodowska-Curie Actions Postdoctoral Fellowship (EP/Z00196X/1); Biotechnology and Biological Sciences Research Council grants BB/Z515115/1; European Research Council (ERC)-Advanced grant PathEVome (787764); and Scottish Government Rural and Environment Science and Analytical Services Division (RESAS) JHI B1-1.

Author contributions

S.W., W.W and P.R.J.B. conceived of and designed the research; S.W. and W.W. performed the research; L.X provided resources of *P. infestans* transformants; L.W. provided technical support; S.W., W.W and P.R.J.B. analysed data; S.W., P.R.J.B., S.C.W. and P.C.B. won funding for the research; and S.W., W.W and P.R.J.B. wrote the paper with input from all co-authors.

The authors declare no competing interest.

References

1. Fry WE, *et al.* Five Reasons to Consider Phytophthora infestans a Reemerging Pathogen. *Phytopathology* **105,** 966-981 (2015).
2. Kamoun S, *et al.* The Top 10 oomycete pathogens in molecular plant pathology. *Mol Plant Pathol* **16,** 413-434 (2015).
3. Tanaka S, Kahmann R. Cell wall-associated effectors of plant-colonizing fungi. *Mycologia* **113,** 247-260 (2021).
4. Kronmiller BA, *et al.* Comparative Genomic Analysis of 31 Phytophthora Genomes Reveals Genome Plasticity and Horizontal Gene Transfer. *Mol Plant Microbe In* **36,** 26-46 (2023).

5. Mandal K, Dutta S, Upadhyay A, Panda A, Tripathy S. Comparative Genome Analysis Across 128 Isolates Reveal Species-Specific Microsatellite Distribution and Localized Evolution of Compartmentalized Genomes. *Frontiers in Microbiology* **13,** (2022).
6. Tör M, Wood T, Webb A, Göl D, McDowell JM. Recent developments in plant-downy mildew interactions. *Seminars in Cell & Developmental Biology* **148,** 42-50 (2023).
7. He Q, McLellan H, Boevink PC, Birch PRJ. All Roads Lead to Susceptibility: The Many Modes of Action of Fungal and Oomycete Intracellular Effectors. *Plant Commun* **1,** 100050 (2020).
8. Petre B, *et al.* Host-interactor screens of Phytophthora infestans RXLR proteins reveal vesicle trafficking as a major effector-targeted process. *Plant Cell* **33,** 1447-1471 (2021).
9. McLellan H, *et al.* Exploiting breakdown in nonhost effector-target interactions to boost host disease resistance. *Proc Natl Acad Sci U S A* **119,** e2114064119 (2022).
10. Wang S, McLellan H, Boevink PC, Birch PRJ. RxLR Effectors: Master Modulators, Modifiers and Manipulators. *Mol Plant Microbe Interact* **36,** 754-763 (2023).
11. Sundaram B, Tweedell RE, Kumar SP, Kanneganti TD. The NLR family of innate immune and cell death sensors. *Immunity* **57,** 674-699 (2024).
12. Whisson SC, *et al.* A translocation signal for delivery of oomycete effector proteins into host plant cells. *Nature* **450,** 115-+ (2007).
13. Wawra S, *et al.* The RxLR Motif of the Host Targeting Effector AVR3a of Phytophthora infestans Is Cleaved before Secretion. *Plant Cell* **29,** 1184-1195 (2017).
14. Xu L, *et al.* Proteolytic processing of both RXLR and EER motifs in oomycete effectors. *New Phytologist* **245,** 1640-1654 (2025).
15. Wang S, Boevink PC, Welsh L, Zhang R, Whisson SC, Birch PRJ. Delivery of cytoplasmic and apoplastic effectors from Phytophthora infestans haustoria by distinct secretion pathways. *New Phytol* **216,** 205-215 (2017).
16. Wang S, Welsh L, Thorpe P, Whisson SC, Boevink PC, Birch PRJ. The Phytophthora infestans Haustorium Is a Site for Secretion of Diverse Classes of Infection-Associated Proteins. *mBio* **9,** (2018).
17. Giraldo MC, *et al.* Two distinct secretion systems facilitate tissue invasion by the rice blast fungus Magnaporthe oryzae. *Nat Commun* **4,** 1996 (2013).
18. Lippincott-Schwartz J, Yuan L, Tipper C, Amherdt M, Orci L, Klausner RD. Brefeldin A's effects on endosomes, lysosomes, and the TGN suggest a general mechanism for regulating organelle structure and membrane traffic. *Cell* **67,** 601-616 (1991).
19. Breen S, *et al.* Identification of MARVELlous protein markers for Phytophthora infestans extracellular vesicles. Preprint at https://www.biorxiv.org/content/10.1101/2025.04.11.648357v2 (2025).
20. Cai Q, *et al.* Message in a Bubble: Shuttling Small RNAs and Proteins Between Cells and Interacting Organisms Using Extracellular Vesicles. *Annu Rev Plant Biol* **72,** 497-524 (2021).
21. He B, *et al.* Fungal small RNAs ride in extracellular vesicles to enter plant cells through clathrin-mediated endocytosis. *Nat Commun* **14,** 4383 (2023).

22. He B, *et al.* RNA-binding proteins contribute to small RNA loading in plant extracellular vesicles. *Nat Plants* **7,** 342-352 (2021).
23. Wang S, *et al.* Plant mRNAs move into a fungal pathogen via extracellular vesicles to reduce infection. *Cell Host Microbe* **32,** 93-105 e106 (2024).
24. Huang YF, *et al.* Rice extracellular vesicles send defense proteins into fungus to reduce disease. *Dev Cell* **60,** (2025).
25. Koch BL, Rutter BD, Borniego ML, Singla-Rastogi M, Gardner DM, Innes RW. Arabidopsis Produces Distinct Subpopulations of Extracellular Vesicles That Respond Differentially to Biotic Stress, Altering Growth and Infectivity of a Fungal Pathogen. *Journal of Extracellular Vesicles* **14,** (2025).
26. Reid G, *et al.* The human multidrug resistance protein MRP4 functions as a prostaglandin efflux transporter and is inhibited by nonsteroidal antiinflammatory drugs. *P Natl Acad Sci USA* **100,** 9244-9249 (2003).
27. Osteikoetxea X, *et al.* Differential detergent sensitivity of extracellular vesicle subpopulations. Org Biomol Chem **13,** 9775-9782 (2015).
28. Cela I, *et al.* KDEL Receptors: Pathophysiological Functions, Therapeutic Options, and Biotechnological Opportunities. *Biomedicines* **10,** (2022).
29. Boevink PC, *et al.* A Phytophthora infestans RXLR effector targets plant PP1c isoforms that promote late blight disease. *Nat Commun* **7,** 10311 (2016).
30. Bentham AR, Wang W, Trusch F, Varden FA, Birch PRJ, Banfield MJ. The WY Domain of an RxLr Effector Drives Interactions with a Host Target Phosphatase to Mimic Host Regulatory Proteins and Promote Infection. *Mol Plant Microbe In* **37,** 239-249 (2024).
31. Orci L, Perrelet A, Ravazzola M, Wieland FT, Schekman R, Rothman JE. Bfa Bodies - a Subcompartment of the Endoplasmic-Reticulum. *P Natl Acad Sci USA* **90,** 11089-11093 (1993).
32. Horrocks P, Muhia D. PEXEL/VTS: a proein-export motif in erythroctytes infected with malaria parasites. *Trends in Parasitology* **21,** 396-399 (2005).
33. Boddey JA, *et al.* Export of malaria proteins requires co-translational processing of the PEXEL motif independent of phosphoinositol-3-phosphate binding. *Nature Comms* **7,** 10470 (2016)
34. Egea PF. Crossing the vacuolar rubicon: structural insights into effector protein trafficking in apicomplexan parasites. *Microorganisms* **8,** 865 (2020).
35. Lin X, *et al.* Divergent Evolution of PcF/SCR74 Effectors in Oomycetes Is Associated with Distinct Recognition Patterns in Solanaceous Plants. *mBio* **11,** (2020).
36. Judelson HS, Tyler BM, Michelmore RW. Transformation of the Oomycete Pathogen, Phytophthora-Infestans. *Mol Plant Microbe In* **4,** 602-607 (1991).
37. Welsh LRJ, Whisson SC. Protoplast Transformation of Phytophthora spp. *Methods Mol Biol* **2892,** 35-47 (2025).
38. Karimi M, Depicker A, Hilson P. Recombinational cloning with plant gateway vectors. *Plant Physiol* **145,** 1144-1154 (2007).

39. Fic E, Kedracka-Krok S, Jankowska U, Pirog A, Dziedzicka-Wasylewska M. Comparison of protein precipitation methods for various rat brain structures prior to proteomic analysis. *Electrophoresis* **31,** 3573-3579 (2010).
40. Wang H, *et al.* Uptake of oomycete RXLR effectors into host cells by clathrin-mediated endocytosis. *Plant Cell* **35,** 2504-2526 (2023).
41. Gilles JF, Dos Santos M, Boudier T, Bolte S, Heck N. DiAna, an ImageJ tool for object-based 3D co-localization and distance analysis. *Methods* **115,** 55-64 (2017).

507 **Figures**

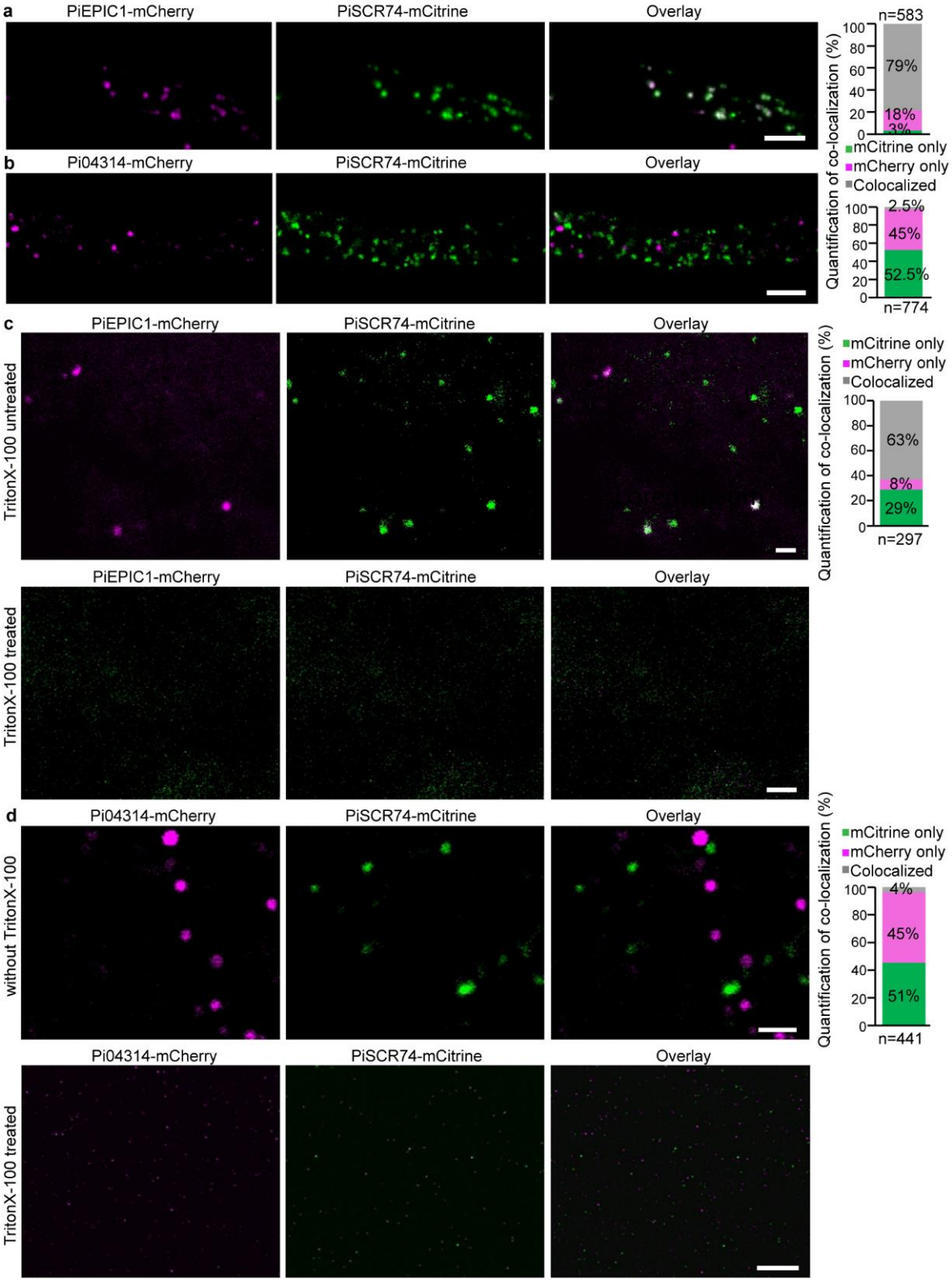

508

509 **Fig. 1| RXLR effectors and apoplastic effectors are associated with different types of**
510 **secretory vesicles. a**, Confocal microscopy images showing colocalization of PiSCR74-
511 mCitrine with PiEPIC1-mCherry in puncta in cultured hyphae. **b**. PiSCR74-mCitrine co-
512 expressed with the RXLR effector Pi04314-mCherry, showing a lack of colocalization in
513 puncta in cultured hyphae. Scale bars, 10 µm (**a**, **b**). **c**, Endosomal vesicles isolated from the

514 same dual transformants shown in **a** confirm colocalization between the apoplastic effectors
515 (upper panel). Treatment with 1% Triton X-100 disrupts vesicle integrity, indicating that the
516 punctate structures are membrane-bound (lower panel). Quantification of colocalization is
517 shown in the accompanying graphs. **d,** Endosomal vesicles isolated from the same dual
518 transformants as in **b** show almost no colocalization between Pi04314 and PiSCR74. Treatment
519 with 1% Triton X-100 confirms both effectors are associated with membrane structures. Scale
520 bars, 2 µm (**c**–**d**). Quantification of colocalization is presented in the accompanying graphs.
521 The numbers of total and colabelled puncta were determined using the DiAna plugin in Fiji (**a**–
522 **d**). n=total puncta.

523

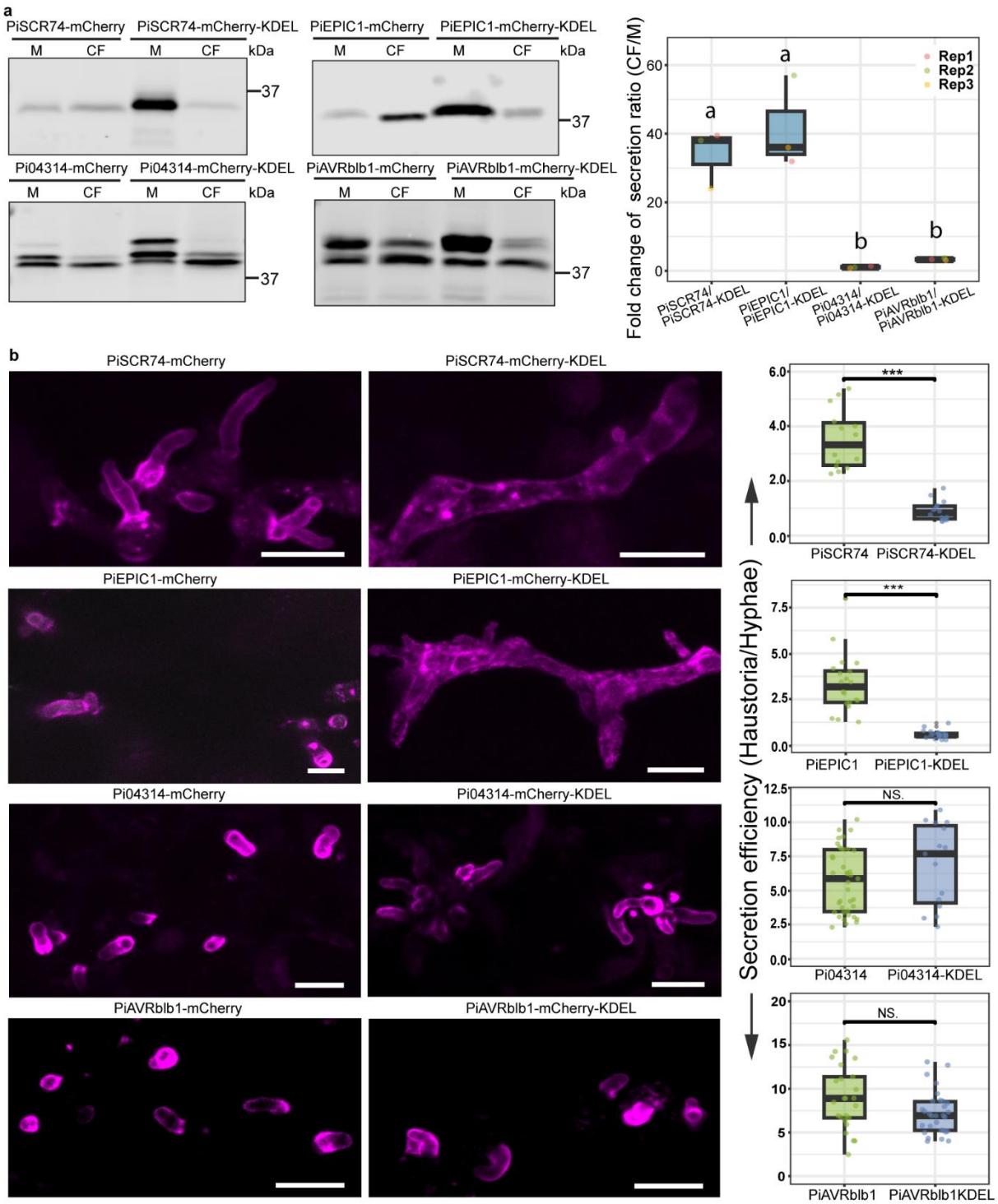

Fig. 2| Apoplastic effectors secreted via Golgi but RXLR effectors take an alternative route.

a, Immunoblot analysis shows retention of apoplastic effector fusions PiSCR74-mCherry and PiEPIC1-mCherry inside mycelia when fused to a KDEL motif, compared to efficient secretion in their unmodified counterparts. In contrast, the secretion efficicy of RXLR effector fusions Pi04314-mCherry and PiAVRblb1-mCherry was not significantly affected by the addition of the KDEL motif. Protein sizes are indicated in kDa. Quantification of the results is presented in the accompanying boxplot, highlighting the significantly greater impact of the KDEL motif on the secretion of apoplastic effectors compared to RXLR effectors. Secretion efficiency was

534 calculated as the ratio of protein intensity in culture filtrate (CF) to that in mycelial extracts
535 (M). Fold changes represent the difference in CF/M ratios between unmodified and KDEL-
536 containing versions. Data are presented as mean ± SD from three biological replicates indicated
537 by small solid circles. Statistical analysis was performed using one-way ANOVA with post-hoc
538 Tukey HSD test to determine significance. **b,** Confocal microscopy images of infectious
539 hyphae in potato leaf tissue showing that the accumulation of PiSCR74-mCherry and PiEPIC1-
540 mCherry at haustoria is markedly reduced when appended with a KDEL motif, compared to
541 their unmodified versions *in planta*. In contrast, accumulation of Pi04314-mCherry and
542 PiAVRblb1-mCherry at haustoria is not significantly affected by the addition of KDEL.
543 Quantification of the results is presented in the accompanying box plots. Secretion efficiency
544 was calculated based on the fluorescence intensity ratio between haustoria and adjacent hyphae
545 area. Data are presented as mean ± SD from three biological replicates. Individual data points
546 are represented by small solid circles. Statistical analysis was performed using student's *t*-test.
547 Scale bars: 10 µm.
548

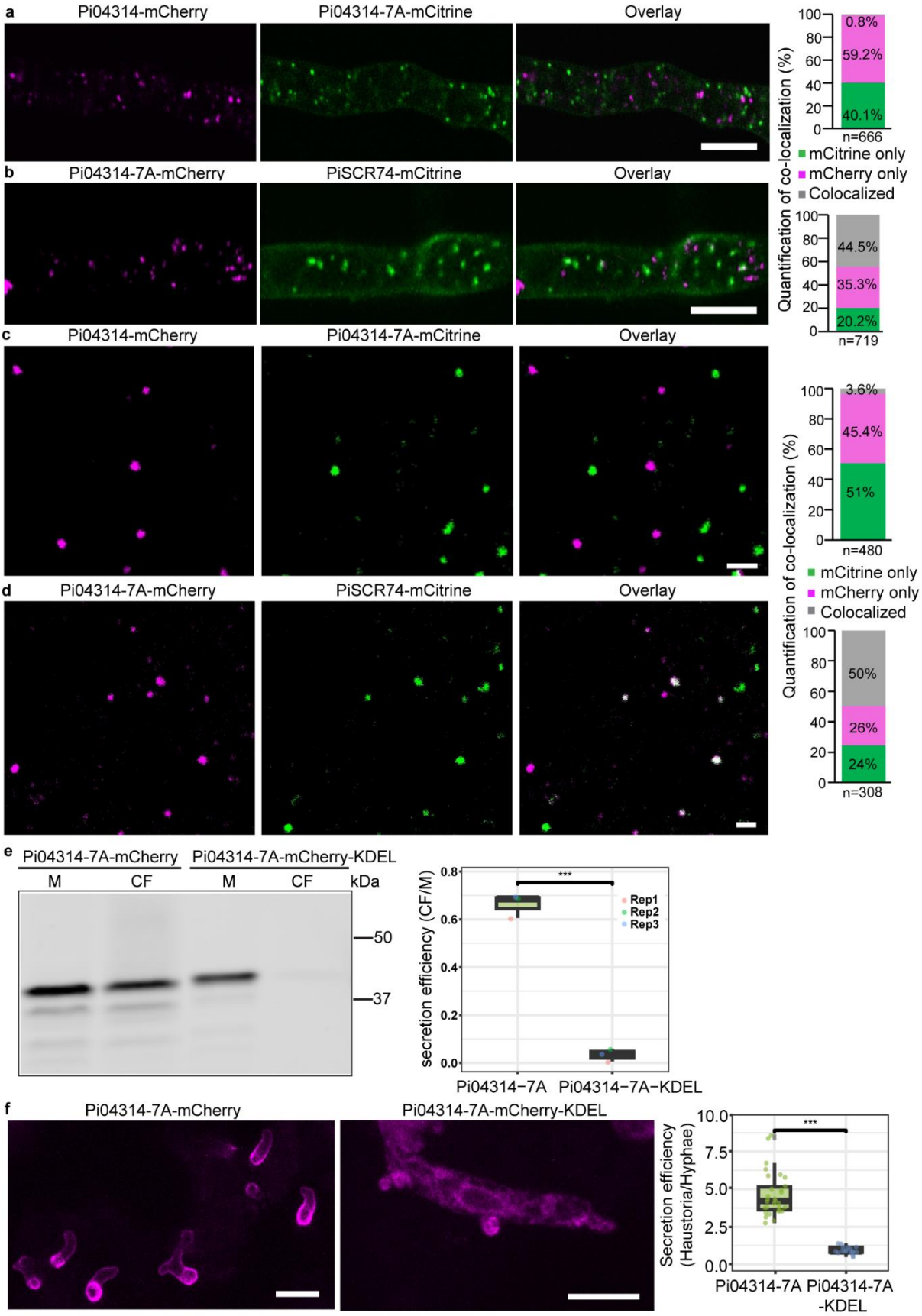
a
Pi04314-mCherry
Pi04314-7A-mCitrine
Overlay
0.8%
59.2%
40.1%
n=666
b
Pi04314-7A-mCherry
PiSCR74-mCitrine
Overlay
44.5%
35.3%
20.2%
n=719
c
Pi04314-mCherry
Pi04314-7A-mCitrine
Overlay
3.6%
45.4%
51%
n=480
d
Pi04314-7A-mCherry
PiSCR74-mCitrine
Overlay
50%
26%
24%
n=308
Quantification of co-localization (%)
mCitrine only
mCherry only
Colocalized
e
Pi04314-7A-mCherry
Pi04314-7A-mCherry-KDEL
M
CF
M
CF
kDa
50
37
secretion efficiency (CF/M)
Rep1
Rep2
Rep3
Pi04314−7A
Pi04314−7A−KDEL
f
Pi04314-7A-mCherry
Pi04314-7A-mCherry-KDEL
Secretion efficiency (Haustoria/Hyphae)
Pi04314-7A
Pi04314-7A -KDEL

549
550
551

552 **Fig. 3| RXLR-EER motifs determine secretion pathways. a**, Confocal microscopy images
553 showing wild-type Pi04314-mCherry does not colocalize with the RXLR mutant effector
554 Pi04314-7A-mCitrine. **b**, In contrast, colocalization of PiSCR74-mCitrine with Pi04314-7A-
555 mCherry was observed in cultured hyphae. Scale bars, 10 µm. **c**, Endosomal vesicles isolated
556 from the same dual transformants as in **a** confirm that Pi04314-7A does not colocalize with
557 wild-type Pi04314. **d**, Confocal microscopy shows colocalization of Pi04314-7A with the
558 apoplastic effector PiSCR74. Quantification of colocalization is shown in the accompanying
559 graphs. The numbers of total (n) and colabelled puncta were determined using the DiAna plugin
560 in Fiji (**a**-**d**). Scale bars, 2 µm. **e**, Immunoblot analysis reveals that Pi04314-7A-mCherry-
561 KDEL is largely retained in the mycelia (M) while secretion of the unmodified variant is readily
562 detected in the culture filtrate (CF). Secretion efficiency was determined by calculating the
563 ratio of protein abundance in the culture filtrate (CF) relative to that in M. Quantification of
564 the protein secretion efficiency is presented in the accompanying boxplot. Data are presented
565 as mean ± SD from three biological replicates indicated by small solid circles. Protein sizes
566 are indicated in kDa. **f**, Confocal microscopy images of infectious hyphae in potato leaf tissue
567 show that Pi04314-7A-mCherry secretion at haustoria is significantly diminished when fused
568 to a KDEL motif, compared to the intense haustorial signal observed with the unmodified
569 version *in planta*. Quantitative analysis is shown in the accompanying boxplots, where
570 secretion efficiency was assessed by calculating the fluorescence intensity ratio between
571 haustoria and hyphae. Data are expressed as mean ± SD from three independent biological
572 replicates, with individual measurements represented by solid dots. Statistical significance was
573 determined using student's *t*-test. *** indicates $p<0.001$ (**e**, **f**). Scale bars, 10 µm.
574
575
576
577
578
579
580
581
582
583
584
585

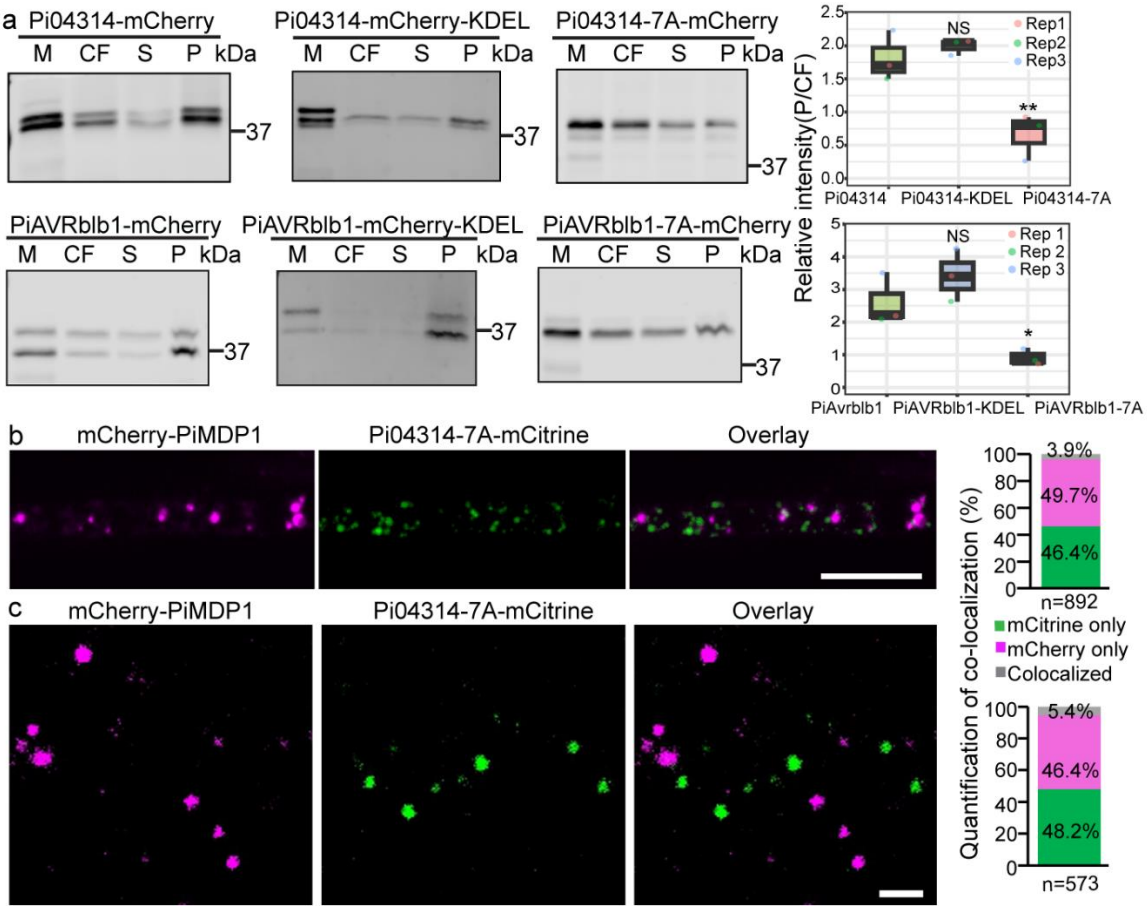

Fig. 4 | RXLR-EER motifs determine the association of effectors with extracellular vesicles (EVs) a, Immunoblot analysis of protein preparations of different fractions from cultured hyphae shows that RXLR effector fusions Pi04314-mCherry, PiAVRblb1-mCherry and their KDEL-modified variants are predominantly enriched in the pellet (P) fraction which contains EVs, whereas the RXLR-EER mutant variant displays markedly reduced association with the pellet fraction. Quantification of protein levels in the pellet fraction relative to that in the culture filtrate (CF) is shown in the accompanying boxplot. Data are expressed as mean ± SD from three independent biological replicates, with individual values represented by solid circles. Statistical analysis was performed using ordinary one-way ANOVA with Dunnett's multiple comparisons test to determine significance. M= mycelia; S=supernatant. Protein sizes are indicated in kDa. **b**, Confocal microscopy images show that mCherry-PiMDP1 and Pi04314-7A-mCitrine do not colocalize in cultured hyphae. Scale bars, 10 µm. **c**, Endosomal vesicles isolated from the same dual transformants as in **b** confirm the absence of colocalization of Pi04314-7A and PiMDP1. Quantitative analysis of colocalization is presented in the accompanying graphs. The total numbers of puncta (n) and colocalized signals were measured using the DiAna plugin in Fiji (**b**, **c**). Scale bars, 2 µm.